Progress In Electromagnetics Research M, Vol. 7, 179–192, 2009

SIMULTANEOUS TE AND TM SURFACE POLARITONS IN A BILAYER COMPOSED OF A SINGLE-NEGATIVE MATERIALS

S. Roshan Entezar

Physics Department
University of Tabriz
Tabriz, Iran

Abstract—We investigate the dispersion properties of both TE and TM surface polariton modes formed at the surfaces of a bilayer composed of a single-negative materials. The dispersion curves of surface polaritons modes is found to consist of two branches, and it is shown that TE and TM surface polaritons may have a simultaneous mode. The characteristics of TE and TM surface polaritons modes (the frequency, localization position, ...) are shown to depend on the relative thicknesses of two single-negative layers of the bilayer. We find that the TE and TM surface polariton modes propagate in the same directions along the interfaces of the bilayer in the most cases. Nevertheless, the TE and TM surface polariton modes may have opposite directions of propagation for appropriate thicknesses of two single-negative layers. This can be interesting especially in the case of simultaneous TE and TM surface polariton mode, for which the structure acts as a polarizing beam splitter.

1. INTRODUCTION

Double negative (DNG) materials with simultaneously negative permittivity and negative permeability have attracted a great deal of attention for their unique properties and useful applications [1–9]. This dates back to 1960s when Veselago first introduced the concept of left-handed material (LHM) with simultaneously negative ε and μ and anticipated their unique electromagnetic properties in theory [10]. Shelby et al. [11], inspired by the work Pendry et al. [12, 13], proposed the first DNG medium by combining periodic arrays of split ring

Corresponding author: S. R. Entezar (s-roshan@tabrizu.ac.ir).

resonators (SRRs) and wire strips and experimentally verified the phenomenon of the negative refraction. Due to the remarkable features of DNG materials, many potential applications have been proposed and studied by many research groups [14–18]. Most of the work reported recently has been focused on the DNG media. However, material in which only one of the two parameters ε and μ has the negative real part, not both, may also possess interesting properties (see e.g., [19–22]). These so-called single-negative (SNG) materials support evanescent wave in order to maintain positive definite energy density. Because ε and μ are frequency dependent, only within a certain frequency range we have epsilon-negative (ENG) media ($\varepsilon < 0$ and $\mu > 0$) or mu-negative (MNG) materials ($\varepsilon > 0$ and $\mu < 0$), which is called the SNG frequency range. Suitably coupled SNG media may offer exciting possibilities in the design of future devices and components, and since only one of their parameters needs to be negative in a given frequency range, it is conceivable that they may conceptually be constructed more easily than DNG media, for which both parameters should possess negative real parts in a given band of frequencies. With the aim to further clarify the interesting properties of SNG, in this paper, the surface polariton modes (SPM) that exist near the boundary of a bilayer composed of MNG-ENG layers have been investigated. These SPMs are those electromagnetic normal modes of the bilayer, which have an evanescent behavior both inside and outside the bilayer and propagate along the interface. Having, in linear case, the field maximum on the interface, the SPMs are a very sensitive and convenient tool for studying of the physical properties of the surfaces. Thus the investigations of SPMs are important from both scientific point of view and practical one [23–25]. In papers [26–29], the SPMs propagating along the interface between vacuum and metallic magnetic medium with simultaneously negative ε and μ were shown to exist. We have analyzed in detail the SPMs in a pair of juxtaposed ENG and MNG slabs, showing interesting properties such as simultaneously TE and TM polarized SPMs with opposite total energy flow directions. Section 2 introduces the model of the system under consideration. In Section 3, the properties of SPMs are studied. Finally, Section 4 concludes with brief comments.

2. THEORETICAL MODEL

We study SPMs dispersion relations for a bilayer of thickness d. The bilayer is composed of a pair of slabs of thicknesses d_1 and d_2, one made of a MNG material and the other of a ENG material inserted in the region $0 < z < d_1 + d_2$. The media at $z < 0$ and $z < d$ are uniform

media of low refractive index, $n_0 = \sqrt{\varepsilon_0 \mu_0}$. The relative permittivity (ε_0) and permeability (μ_0) of the uniform medium are assumed to be frequency independent. Consider the relative permittivity and the permeability in MNG materials are given by:

$$\varepsilon_1 = 3, \quad \mu_1 = 1 - \frac{\omega_{mp}^2}{f^2 + if\Gamma_m} \tag{1}$$

and those in ENG materials are given by

$$\varepsilon_2 = 1 - \frac{\omega_{ep}^2}{f^2 + if\Gamma_e}, \quad \mu_2 = 1.2 \tag{2}$$

Here, f is the frequency; ω_{mp}, ω_{ep} are the magnetic and electronic plasma frequencies, respectively. Both Γ_m and Γ_e are the dissipation factor. Note that these kinds of dispersion may be realized in special microstrips [12, 30, 31]. For instance, loops of conducting wires have the magnetic plasma properties, and the permeability is described by the first equation. On the other hand, a metallic microstructure containing a regular arrays of thin wires is able to behave like a plasma with the resonant frequency ω_{ep} at GHz region. As a consequence, the dielectric response of such a plasma can be described by the second equation. The frequency f in the above equations is measured in GHz. Here we assume $\omega_{mp} = 10\,\text{GHz}$, $\omega_{me} = 12\,\text{GHz}$ and $\Gamma_m = \Gamma_e = 0.03f$. In this case, the frequency range in which both μ_1 and ε_2 are negative extend up to $\omega_{mp} = 10\,\text{GHz}$. For the medium at $x < 0$ and $x > d$ we assume $\varepsilon_0 = 1$ and $\mu_0 = 1$. By choosing a coordinate system in which the layers have normal vector along OZ, the electric (magnetic) field of TE-polarized (TM-polarized) SPMs (which is shown by F) will be parallel to the OY axis. We consider the field in the region $z < 0$ has the form

$$\vec{F}^{(0)} = \hat{e}_y A e^{k_{0z} z} e^{ik_x x} \tag{3}$$

Here, $\hat{e}_y$ is unit vectors in the y direction; $k_{0z} = \sqrt{k_x^2 - k^2 \varepsilon_0 \mu_0}$; k_x is the (constant) x-component of the wavevector; $k = \frac{\omega}{c}$ and $\omega = 2\pi f$. The field in the region $0 < z < d_1$ is given by

$$\vec{F}^{(1)} = \hat{e}_y \left(C_1 e^{k_{1z} z} + D_1 e^{-k_{1z} z} \right) e^{ik_x x} \tag{4}$$

where $k_{1z} = \sqrt{k_x^2 - k^2 \varepsilon_1 \mu_1}$ and for the field in the region $d_1 < z < d$ we use

$$\vec{F}^{(2)} = \hat{e}_y \left(C_2 e^{k_{2z} z} + D_2 e^{-k_{2z} z} \right) e^{ik_x x} \tag{5}$$

where $k_{2z} = \sqrt{k_x^2 - k^2 \varepsilon_2 \mu_2}$.

In the region $z > d$ the field is written in the form

$$\vec{F}^{(3)} = \hat{e}_y B e^{-k_{0z}(z-d)} e^{ik_x x} \tag{6}$$

Applying the boundary conditions

$$F^{(i)} = F^{(j)} \tag{7}$$

$$\frac{1}{\alpha_i}\frac{dF^{(i)}}{dz} = \frac{1}{\alpha_j}\frac{dF^{(j)}}{dz} \tag{8}$$

at the interfaces of the structure yields a system of six homogeneous equations. Here, $i, j = 0, 1, 2$ and α_i is μ_i (ε_i) in the case of the TE-polarized (TM-polarized) SPM. By solving this system of equations, we can obtain the dispersion relation for TE-polarized (TM-polarized) SPMs by numerically solving the following dispersion condition

$$\frac{\kappa_{21}+\tanh(k_{1z}d_1)\tanh(k_{2z}d_2)+\kappa_{01}\tanh(k_{2z}d_2)+\kappa_{02}\tanh(k_{1z}d_1)}{1+\kappa_{21}\tanh(k_{1z}d_1)\tanh(k_{2z}d_2)+\kappa_{02}\tanh(k_{2z}d_2)+\kappa_{01}\tanh(k_{1z}d_1)} = \kappa_{01} \tag{9}$$

where $\kappa_{ij} = \frac{k_{iz}}{k_{jz}}\frac{\alpha_j}{\alpha_i}$. For the SPMs the field amplitudes decay in an exponential fashion as one moves away from the interfaces. Therefore, we assume $k_x > kn_0$ in what follow.

3. RESULTS AND DISCUSSION

In order to discuss the dispersion properties of the SPMs we numerically solved Eq. (9) and plotted the dispersion curves of the TE and TM polarized SPMs as a function of $\beta = k_x = k$ in Fig. 1. Here, three different cases are considered for the thicknesses of the MNG and the ENG layers of the bilayer with thickness $d = d_1 + d_2 = \frac{1}{2}\frac{c}{\omega_{mp}}$. As one can see from Fig. 1, the dispersion curves of TE-polarized (solid lines) and TM-polarized (dashed lines) SPMs consist of two branches. Depending on the relative thicknesses of the MNG ($\frac{d_1}{d}$) and the ENG ($\frac{d_2}{d}$) layers of the bilayer, the TE- and the TM-polarized SPM dispersion curves of the upper or lower branch may intersect with each other. For these modes, the structure can support both TE- and TM-polarized SPMs simultaneously. In other words, for these modes we can have unpolarized surface polaritons. As mentioned earlier, the frequency of simultaneous TE- and TM-polarized SPMs depends on the relative thicknesses of the MNG and the ENG layers of the bilayer. To indicate this, in Fig. 2, the dispersion curves of TE- (solid lines) and TM-polarized (dotted lines) SPMs are plotted as a function of

d_2/d (the thickness of ENG layer to the width of the bilayer) for two different β. As one can see from Fig. 2, the structure can support simultaneous TE- and TM-polarized SPMs for appropriate choice of the parameters d_1, d_2 and β.

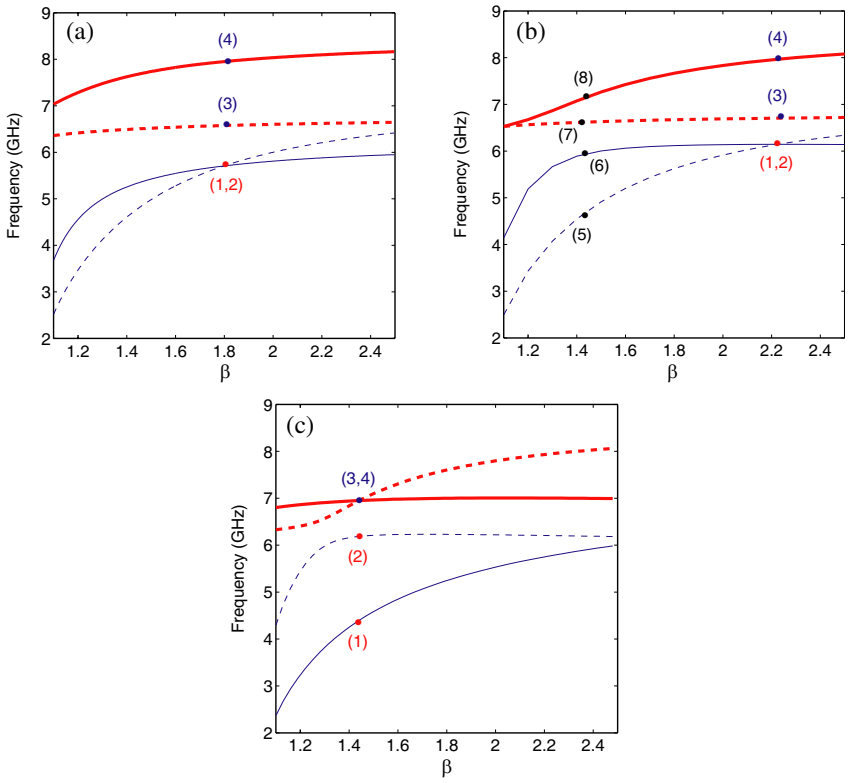

Figure 1. Dispersion property of TE (solid lines) and TM (dashed lines) polarized SPMs as a function of β for the cases of (a) $d_1 = \frac{1}{3}d$, $d_2 = \frac{2}{3}d$, (b) $d_1 = d_2 = \frac{1}{2}d$ and (c) $d_1 = \frac{2}{3}d$, $d_2 = \frac{1}{3}d$. Here, $d = \frac{1}{2}\frac{c}{\omega_{mp}}$.

The existence of two branches for either polarization of SPMs in the bilayer structure can be explained using perturbation theory [32]. According to this theory, the bilayer structure with layers of different refractive indices and thicknesses can be considered as a system of two interacting waveguides. The number of eigenvalues of the interacting waveguides is equal to the number of waveguides. The interaction strength between the waveguides depends on the separation between the waveguides. When the separation is infinite, there is no interaction, and the waveguides can be considered as independent of each other

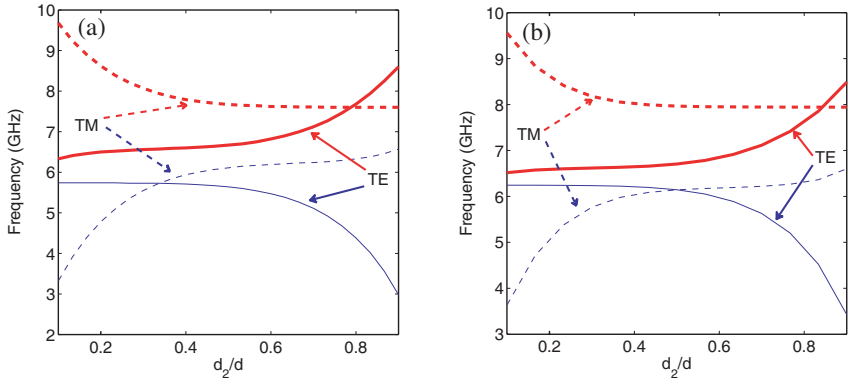

Figure 2. The dispersion curves of TE (solid lines) and TM (dotted lines) polarized SPMs as a function of d_2/d for (a) $\beta = 1.81$ and (b) $\beta = 2.22$. Here $d_1 = d - d_2$.

with two independent eigenvalues. As the waveguides are brought together, the interaction between the waveguides causes the eigenvalues to be dependent. Since the electromagnetic fields have evanescent nature in the SNG materials, these two modes are localized near the interfaces of bilayer structure. Due to this evanescent nature, they will not interact directly with an incoming plane waves. So, they can be excited by the total internal reflection (ATR) method. The so-called Otto configuration [33] (prism-air gap-dielectric) is used to study the excitation of SPMs, replacing a dielectric or a metal by a bilayer composed of MNG and ENG materials (see Fig. 1) [34–36]. In the present paper, the spectral reflectivity is studied to obtain the dispersion relation of the SPMs using ATR method. This method is a powerful technique for the study of non-radiative surface excitations in thin films or surfaces [37, 38]. For a given frequency, non-radiative surface waves have a wave vector parallel to the surface that is larger than any of the corresponding wave vectors at both media forming the surface. In order to coupling light with the surface modes, we need a way to increase the wave vector of the light incident at the interface. That is the purpose of the ATR setup. It is obtained by using a prism joined to the system as illustrated in Fig. 3(a). The radiation is incident from the left hand side, at an angle of incidence θ, in a medium (usually a prism) having relative permittivity and permeability $\acute{\varepsilon}$ and $\acute{\mu}$. A film of thickness d_a and relative permittivity and permeability ε_0 and μ_0 acts as a spacer between the prism and the bilayer. If the angle of incidence is such that $\beta = \sqrt{\acute{\varepsilon}\acute{\mu}}\sin(\theta) > \sqrt{\varepsilon_0\mu_0}$, the electromagnetic field will penetrate the gap as an evanescent wave, which can interact

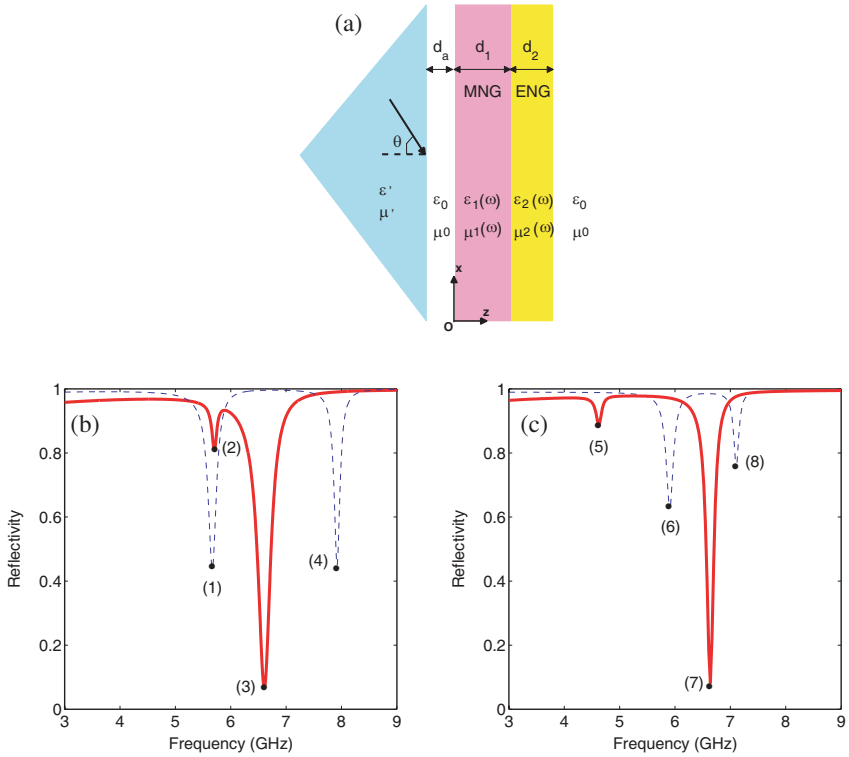

Figure 3. (a) Geometry of ATR experiment. The calculated ATR spectrum of TE (solid line) and TM (dashed line) polarizations for (b) $d_1 = \frac{1}{3}d$, $d_2 = \frac{2}{3}d$, $\beta = 1.79$ and (c) $d_1 = d_2 = \frac{1}{2}d$, $\beta = 1.42$.

with the evanescent SPMs. The TE and TM polarized ATR spectrums for the bilayer with $d_1 = d_2 = \frac{1}{2}d$ and given β are shown in Figs. 3(b), (c). Two dips in each ATR spectrums are due to two SPMs for each polarization. Here, points $(1, 2, 3, 4)$ and $(5, 6, 7, 8)$ correspond to the modes in Figs. 1(a), (b), respectively. As one can see from Fig. 3(b), both TE and TM polarized ATR spectrums have a dip at the same frequency and β (points $1, 2$). So, for the given parameters, the structure can support TE and TM polarized SPMs, simultaneously.

As mentioned above, two dips in the ATR spectrum of each polarization correspond to two SPMs. Our investigations show that the transverse structures of these modes are different. To show this, the transverse structure and the intensity distribution of the TE- and TM-polarized SPMs are plotted in Figs. 4, 5, to the points $1, 2, 3, 4$ in

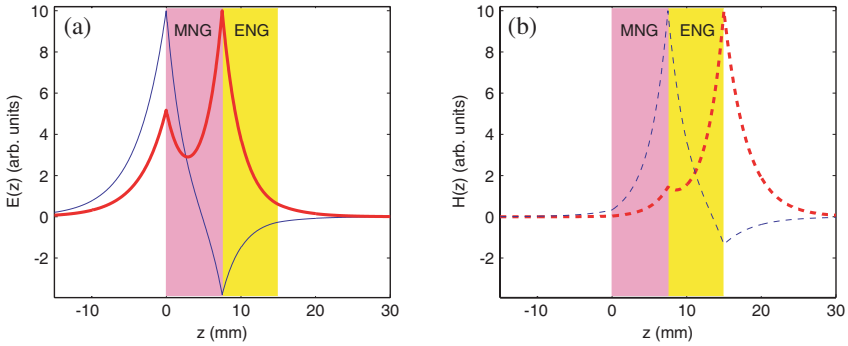

Figure 4. The transverse profile of (a) the TE polarized SPMs and (b) TM polarized SPMs vs coordinate z. Here, the modes are correspond to the points 1 (the thin solid line), 2 (the thin dashed line), 3 (the thick dashed line) and 4 (thick solid line) in Fig. 1(b), respectively. The other parameters are $d_1 = d_2 = \frac{1}{2}d$ and $\beta = 2.22$.

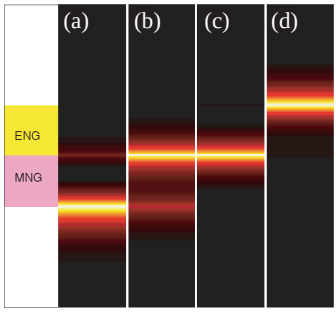

Figure 5. The intensity distribution of the TE and TM polarized SPMs correspond to the points (a) 1, (b) 2, (c) 3 and (d) 4 in Fig. 1(b), respectively. Here $d_1 = d_2 = \frac{1}{2}d$ and $\beta = 2.22$.

Fig. 1(b). As one can see from Fig. 4, TE (TM) polarized SPMs from the upper or the lower branches of the dispersion curves have different transverse structures. Fig. 5 indicates that the peak intensity of the TE (TM) polarized SPMs is at the left surface of the MNG (ENG) layer and/or right surface of the MNG (ENG) layer. Our investigations show that the peak intensity can be switched from one surface of the MNG (ENG) layer to the other surface by tuning the parameter β. For the peak intensity between MNG and ENG layers, the bilayer acts as a

waveguide. In order to reveal the guidance ability of the bilayer, the integrated energy density over the width of the bilayer ($U_{Bilayer}$) to the total energy density (U_{Total}) for SPMs is plotted as a function of β in Fig. 6. Here, the modes correspond to those in Fig. 1(b). The total energy density associated with the whole mode is determined by an integration over z coordinate as

$$U_{Total} = \int_{-\infty}^{\infty} U dz \tag{10}$$

with $U = \frac{1}{16\pi}(\varepsilon|E|^2 + \mu|H|^2)$.

As one can see from Fig. 6, for $\beta > 1.5$ the modes from the upper (lower) branch of the TE (TM) polarized SPMs are more localized at the bilayer. This shows that the bilayer structure composed of MNG and ENG layers has the ability to guide TE and TM polarized SPMs. Our investigations show that the energy flow velocity of SPMs can be positive or negative depending on the relative thicknesses of the MNG and ENG layers. To show this, in Fig. 7, the energy flow velocity of the SPMs is plotted as a function of β for two different cases of a) $d_1 = \frac{1}{3}d$, $d_2 = \frac{2}{3}d$ and b) $d_1 = d_2 = \frac{1}{2}d$. Here, the points $1, 2, 3$ and 4 are correspond to those in Figs. 1(a), (b). It is well known that the energy flow velocity v_E relates total energy flow S_{Total} to the total energy density as $v_E = \frac{S_{Total}}{U_{Total}}$. The corresponding total energy flow associated with the whole mode is determined by an integration over z coordinate as

$$S_{Total} = \int_{-\infty}^{\infty} S dz \tag{11}$$

where $S = \frac{c}{8\pi}\mathrm{Re}[E \times H^*]$.

As one can see from Fig. 7(a), the energy flow velocities v_E of all TE and TM polarized SPMs are positive for the case $d_1 = \frac{1}{3}d$, $d_2 = \frac{2}{3}d$. In other words, all SPMs are forward modes for this choice of the parameters. So, for the modes corresponding to points $(1, 2)$ in Fig. 1(a), the bilayer can support unpolarized SPMs. On the other hand, Fig. 7(b) shows that some TM polarized modes have negative energy flow velocities. Accordingly, the bilayer can support both forward and backward SPMs for the case of $d_1 = d_2 = \frac{1}{2}d$. It is interesting to note that the directions of the energy flow velocities are opposite for the simultaneous TE and TM polarized SPMs corresponding to the points $(1, 2)$ in Fig. 1(b). So, the bilayer can be used as a polarizing beam splitter for this choice of the parameters. In this case, the TE polarized SPM propagates in the forward direction, and the TM polarized SPM propagates in the backward direction along the interfaces of the bilayer.

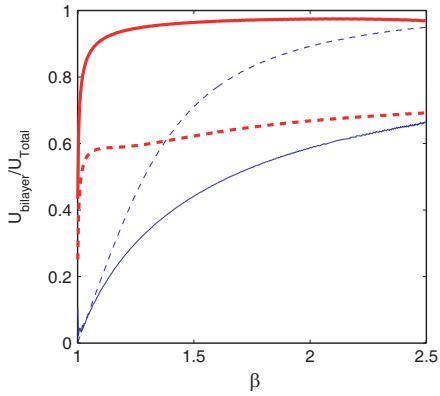

Figure 6. The normalized integrated energy density of the TE (solid lines) and TM (dotted lines) polarized SPMs (corresponding to the modes in the Fig. 1(b)) as a function of β for the case of $d_1 = d_2 = \frac{1}{2}d$.

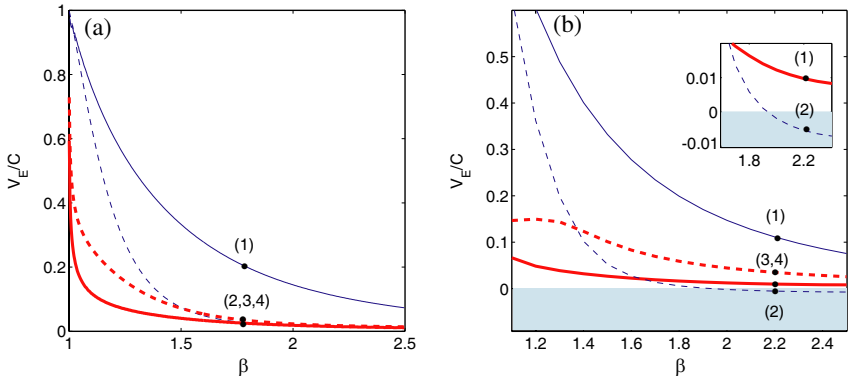

Figure 7. The energy flow velocity of TE (solid lines) and TM (dotted lines) polarized SPMs as a function of β for the cases of (a) $d_1 = \frac{1}{3}d$, $d_2 = \frac{2}{3}d$ and (b) $d_1 = d_2 = \frac{1}{2}d$.

4. CONCLUSION

We have investigated the dispersion properties of TE and TM polarized SPMs formed at the surfaces of a bilayer composed of MNG-ENG layers. In the SNG frequency range, the dispersion curves of both TE and TM polarized surface polariton modes have two branches. The modes from these two branches have different transverse structures with the peak intensity at different interfaces of the bilayer. We

have shown that the peak intensity of the SPMs can be switched from one interface of the bilayer to the other interfaces by tuning the x-component of the wavevector. Moreover, we have revealed that dispersion curves of TE and TM polarized surface polariton modes may intersect with each other depending on the thicknesses of MNG and ENG layers of the bilayer. For these modes the bilayer structure can support simultaneous TE and TM polarized surface polaritons. Depending on the thicknesses of MNG and ENG layers, the simultaneous TE and TM polarized SPMs may have opposite energy flow directions along the interfaces of the bilayer. So, in this case the bilayer can be used as a polarizing beam splitter.

REFERENCES

1. Ziolkowski, R. and E. Heyman, "Wave propagation in media having negative permittivity and permeability," *Phys. Rev. E*, Vol. 64, 056625, 2001.
2. Oliner, A. A., "A periodic-structure negative-refractive-index medium without resonant elements," *IEEE-APS/URSI Int'l Symp. Digest*, 41, June 2002.
3. Sanada, A., C. Caloz, and T. Itoh, "Characteristics of the composite right/left-handed transmission lines," *IEEE Microw. Wirel. Compon. Lett.*, Vol. 14, 68–70, 2004.
4. Caloz, C. and T. Itoh, "Transmission line approach of left-handed (LH) materials and microstrip implementation of an artificial LH transmission line," *IEEE Trans. Antennas Propagat.*, Vol. 52, 1159–1166, 2004.
5. Okabe, H., C. Caloz, and T. Itoh, "A compact enhanced-bandwidth hybrid ring using a left-handed transmission line," *IEEE Trans. Microw. Theory Tech.*, Vol. 52, 798–804, 2004.
6. Ding, W., L. Chen, and C.-H. Liang, "Characteristics of electromagnetic wave propagation in biaxially anisotropic left-handed materials," *Progress In Electromagnetics Research*, PIER 70, 37–52, 2007.
7. Chen, L., W. Ding, X. J. Dang, and C. H. Liang, "Counter-propagating energy-flows in nonlinear left-handed metamaterials," *Progress In Electromagnetics Research*, PIER 70, 257–267, 2007.
8. Xu, W., L. W. Li, H. Y. Yao, T. S. Yeo, and Q. Wu, "Left-handed material effects on waves modes and resonant frequencies: Filled waveguide structures and substrate-loaded patch antennas," *Journal of Electromagnetic Waves and Applications*, Vol. 19, No. 15, 2033–2047, 2005.

9. Grzegorczyk, T. M. and J. A. Kong, "Review of left-handed metamaterials: Evolution from theoretical and numerical studies to potential applications," *Journal of Electromagnetic Waves and Applications*, Vol. 20, No. 14, 2053–2064, 2006.
10. Veselago, V. G., "The electrodynamics of substances with simultaneously negative values of ε and μ," *Soviet Physics USPEKI*, Vol. 10, 509–514, 1968.
11. Shelby, R. A., D. R. Smith, and S. Schultz, "Experimental verification of a negative index of refraction," *Science*, Vol. 292, 77–79, 2001.
12. Pendry, J. B., A. J. Holden, D. J. Robbins, and W. J. Stewart, "Magnetism from conductors and enhanced nonlinear phenomena," *IEEE Trans. Microwave Theory and Techniques*, Vol. 47, 2075–2084, 1999.
13. Pendry, J. B., A. J. Holden, W. J. Stewart, and I. Youngs, "Extremely low frequency plasmons in metallic mesostructures," *Phys. Rev. Lett.*, Vol. 76, 4773–4776, 1996.
14. Caloz, C. and T. Itoh, "Application of the transmission line theory of left-handed (LH) materials to the realization of a microstrip LH line," *IEEE-APS Int'l Symp. Digest*, Vol. 2, 412–415, 2002.
15. Lin, I. H., M. DeVincentis, C. Caloz, and T. Itoh, "Arbitrary duad-band components using composite right/left-handed transmission lines," *IEEE Trans. Microwave Theory Techniques*, Vol. 52, 1142–1149, 2004.
16. Liang, L., B. Li, S.-H. Liu, and C.-H. Liang, "A study of using the double negative structure to enhance the gain of rectangular waveguide antenna arrays," *Progress In Electromagnetics Research*, PIER 65, 275–286, 2006.
17. Hamid, A.-K., "Axially slotted antenna on a circular or elliptic cylinder coated with metamaterials," *Progress In Electromagnetics Research*, PIER 51, 329–341, 2005.
18. Sharma, R., T. Chakravarty, S. Bhooshan, and A. B. Bhattacharyya, "Design of a novel 3 dB microstrip backward wave coupler using defected ground structure," *Progress In Electromagnetics Research*, PIER 65, 261–273, 2006.
19. Alù, A. and N. Engheta, "Guided modes in a waveguide filled with a pair of single-negative (SNG), double-negative (DNG), and/or double-positive (DPS) layers," *IEEE Trans. on Microwave Theory and Techniques*, Vol. 52, 199–210, 2004.
20. Alù, A. and N. Engheta, "Pairing an epsilon-negative slab with a mu-negative slab: Anomalous tunneling and transparency," *IEEE*

Trans. on Antennas and Propagation, Vol. 51, 2558–2570, 2003.

21. Dai, X.-W., M. Yao, X.-J. Dang, and C.-H. Liang, "Transparency of a pair of epsilon-negative slab and mu-negative slab," *Progress In Electromagnetics Research*, PIER 69, 237–246, 2007.
22. Bilotti, F., A. Alu, N. Engheta, and L. Vegni, "Anomalous properties of scattering from cavities partially loaded with double-negative or single-negative metamaterials," *Progress In Electromagnetics Research*, PIER 51, 49–63, 2005.
23. Agranovich, V. M. and D. L. Mills, *Surface Polaritons: Electromagnetic Waves at Surfaces and Interfaces*, North-Holland, Amsterdam, 1982.
24. McGilp, J. F., D. Weaire, and C. H. Patterson, *Epioptics: Linear and Nonlinear Optical Spectroscopy of Surfaces and Interfaces*, Springer-Verlag, Berlin, 1995.
25. Raether, H., *Surface Plasmons*, Springer-Verlag, Heidelberg, 1988.
26. Camley, R. E. and D. L. Mills, "Surface polaritons on uniaxial antiferromagnets," *Phys. Rev. B*, Vol. 26, 1280–1287, 1982.
27. Ruppin, R., "Surface polaritons of left-handed medium," *Phys. Lett. A*, Vol. 277, 61–64, 2000.
28. Ruppin, R., "Surface polaritons of left-handed material slab," *J. Phys: Condens. Matter*, Vol. 13, 1811–1819, 2001.
29. Bespyatykh, Y. I., A. S. Bugaev, and I. E. Dikshtein, "Surface polaritons in composite media with time dispersion of permittivity and permeability," *Phys. Sol. State*, Vol. 43, 2043–2047, 2001.
30. Pendry, J. B., A. J. Holden, D. J. Robbins, and W. J. Stewart, "Low frequency plasmons in thin-wire structures," *J. Phys.: Condens. Matter*, Vol. 10, 4785–4809, 1998.
31. Pendry, J. B., "Negative refraction makes a perfect lens," *Phys. Rev. Lett.*, Vol. 85, 3966–3969, 2000.
32. Yeh, P., A. Yariv, and C. S. Hong, *J. Opt. Soc. Am.*, Vol. 67, 423, 1977.
33. Otto, A., "Excitation of nonradiative surface plasma waves in silver by the method of frustrated total reflection," *Z. Phys.*, Vol. 216, 398–410, 1968.
34. Shadrivov, I. V., R. W. Ziolkowski, A. A. Zharov, and Y. S. Kivshar, "Excitation of guided waves in layered structures with negative refraction," *Opt. Express*, Vol. 13, 481–492, 2005.
35. Dragila, R., B. Luther-Davies, and S. Vukovic, "High transparency of classically opaque metallic films," *Phys. Rev. Lett.*, Vol. 55, 1117–1120, 1985.
36. Vukovic, S. M., N. B. Aleksic, and D. V. Timotijevic, "Anomalous

lateral beam shift and total absorption due to excitation of surface waves in materials with negative refraction," *Eur. Phys. J. D*, Vol. 39, 295–301, 2006.

37. Galli, M., D. Bajoni, M. Patrini, G. Guizzetti, D. Gerace, L. C. Andreani, M. Belotti, and Y. Chen, "Excitation of radiative and evanescent defect modes in linear photonic crystal waveguides," *Phys. Rev. B*, Vol. 70, 081307–4, 2004.
38. Galli, M., M. Belotti, D. Bajoni, M. Patrini, G. Guizzetti, D. Gerace, M. Agio, L. C. Andreani, and Y. Chen, "Single-mode versus multimode behavior in silicon photonic crystal waveguides measured by attenuated total reflectance," *Phys. Rev. B*, Vol. 72, 125322–10, 2005.